Vol 17 No 3, March 2008
1674-1056/2008/17(03)/0943-07
Chinese Physics B
© 2008 Chin. Phys. Soc.
and IOP Publishing Ltd

Nonparaxial propagation of phase-flipped Gaussian beams*

Gao Zeng-Hui(高曾辉)[a)b)c)†] and Lü Bai-Da(吕百达)[c)]

[a)] *Key Laboratory of Computational Physics, Yibin University, Yibin* 644000, *China*
[b)] *Institute of Optoelectronic Information, Yibin University, Yibin* 644000, *China*
[c)] *Institute of Laser Physics and Chemistry, Sichuan University, Chengdu* 610064, *China*

(Received 27 April 2007; revised manuscript received 25 June 2007)

This paper derives the closed-form expressions for nonparaxial phase flipped Gaussian (PFG) beams propagating in free space, through a knife edge and an aperture, which enable us to study nonparaxial propagation properties of PFG beams and to compare nonparaxial results with paraxial ones. It is found that the f parameter, offsetting distance of the knife edge and truncation parameter affect the nonparaxial beam propagation properties. Only under certain conditions the paraxial approximation is applicable. The results are illustrated by numerical examples.

Keywords: nonparaxial propagation, phase flipped Gaussian (PFG) beam, f parameter, offsetting distances

PACC: 4200

1. Introduction

Recently Delaubert *et al*[1] proposed the phase flipped Gaussian (PFG) beam, which has a Gaussian intensity distribution with a π phase flip between the two halves of the beam profile and demonstrates its potential applications in tilt locking of an optical cavity and high precision position measurements. PFG beams can be produced experimentally by means of interferometric and wave plate techniques. Within the framework of the paraxial approximation the propagation properties of PFG beams were studied both by expanding the flipped mode into an infinite sum of odd Hermite–Gauss modes and by using the generalized Huygens–Fresnel integral (Collins formula).[1,2] However, just like Gaussian beams, the paraxial approximation is no longer valid when the beam width is comparable with the wavelength and/or the far-field divergence angle is large enough.[3−7] For such a case the nonparaxial approach has to be taken into consideration. In this paper, based on the Rayleigh–Sommerfeld diffraction integral, analytical propagation equations of nonparaxial PFG beams are derived and their nonparaxial propagation properties are studied and compared with paraxial ones. The results are illustrated by numerical examples.

2. Theoretical formulations

For our study the two-dimensional representation (x, z) of PFG beams in Refs.[1] and [2] is extended to the three-dimensional case (x, y, z) due to the non-separability of the x and y variables.[8] Assume that the field of a PFG beam at the plane z=0 in the Cartesian coordinate system takes the form

$$E_{f.0}(x_0, y_0, 0) = \theta(x_0)\,\theta(y_0)\,E_0(x_0, y_0, 0);$$

$$\theta(x_0) = \begin{cases} -1, & x_0 < 0, \\ 1, & x_0 \geq 0, \end{cases}$$

$$\theta(y_0) = \begin{cases} -1, & y_0 < 0, \\ 1, & y_0 \geq 0, \end{cases} \tag{1}$$

where

$$E_0(x_0, y_0, 0) = \frac{\sqrt{2/\pi}}{w_0} \exp\left(-\frac{x_0^2 + y_0^2}{w_0^2}\right), \tag{2}$$

w_0 denotes the waist width, $\dfrac{\sqrt{2/\pi}}{w_0}$is the normalization factor. It is well known that the strict solution of the Helmholtz equation in the half space $z > 0$ is given by the Rayleigh–Sommerfeld diffraction integral

*Project supported by the National Natural Science Foundation of China (Grant No 10574097).
†Corresponding author. E-mail: dzxx3545065@163.com

of the form.[9]

$$E_{f.0}(\boldsymbol{r}) = -\frac{1}{2\pi}\int\int_{-\infty}^{\infty} E_{f.0}(x_0, y_0, 0) \times \frac{\partial G(\boldsymbol{r}, \boldsymbol{r}_0)}{\partial z}\mathrm{d}x_0\mathrm{d}y_0, \quad (3)$$

where $\boldsymbol{r}_0 = x_0\boldsymbol{i}+y_0\boldsymbol{j}$, $\boldsymbol{r} = x\boldsymbol{i}+y\boldsymbol{j}+z\boldsymbol{k}$, $\boldsymbol{i}, \boldsymbol{j}, \boldsymbol{k}$ are unite vectors in the x, y and z directions, respectively, and

$$G(\boldsymbol{r}, \boldsymbol{r}_0) = \frac{\exp\left(ik|\boldsymbol{r}-\boldsymbol{r}_0|\right)}{|\boldsymbol{r}-\boldsymbol{r}_0|}, \quad (4)$$

k is the wave number related to the wavelength λ by $k = 2\pi/\lambda$.

Expanding $G(\boldsymbol{r}, \boldsymbol{r}_0)$ into

$$G(\boldsymbol{r}, \boldsymbol{r}_0) \approx \frac{1}{r}\exp\left[\mathrm{i}k\left(r + \frac{x_0^2+y_0^2-2xx_0-2yy_0}{2r}\right)\right], \quad (5)$$

recalling the integral formula

$$\int_a^{\infty}\exp\left(-ps^2\right)\sin(qs)\mathrm{d}s = \frac{-\mathrm{i}\sqrt{\pi}}{4\sqrt{p}}\exp\left(-\frac{q^2}{4p}\right)\left[\mathrm{erf}\left(\frac{\mathrm{i}q}{2\sqrt{p}}+a\sqrt{p}\right)a + \mathrm{erf}\left(\frac{\mathrm{i}q}{2\sqrt{p}}-a\sqrt{p}\right)\right], \quad (6)$$

and substituting Eqs.(1) and (5) into Eq.(3), by tedious but straightforward integral calculations we get

$$E_{f.0}(x, y, z) = E_0(x, y, z)\mathrm{erf}\left(\alpha x\right)\mathrm{erf}\left(\alpha y\right), \quad (7)$$

where

$$E_0(x, y, z) = \frac{z/r}{1+\mathrm{i}r/z_0}\frac{\sqrt{2/\pi}}{w_0}\exp\left(\mathrm{i}kr\right) \times \exp\left[\alpha^2\left(x^2+y^2\right)\right], \quad (8)$$

$$\alpha = \mathrm{i}/\left(w_0\sqrt{\left(r/z_0\right)^2 - \mathrm{i}r/z_0}\right), \quad (9)$$

and $r = \sqrt{x^2+y^2+z^2}$, and erf$(\cdot)$ denotes the error function, and $z_0 = \pi w_0^2/\lambda$ is the Rayleigh length. Equation (8) is the propagation formula of nonparaxial Gaussian beams in free space, and apart from a normalization factor it is consistent with Eq.(10a) by letting $w_{0x} = w_{0y}$ in Ref.[6]. Equation (7) indicates that due to the flipped phase, the amplitude and phase of the field $E_0(x,\ y,\ z)$ are modulated by error functions of erf(αx) and erf(αy) of complex argument. It is noted that the x and y variables in Eq.(7) are not separable, which is the general feature of nonparaxial beams.[8]

Under the far-field approximation

$$|\boldsymbol{r}-\boldsymbol{r}_0| \approx r - \frac{xx_0+yy_0}{r}, \quad (10)$$

the substitution from Eqs.(5) and (10) into Eq.(3) leads to

$$E_{ff.0}(x, y, z) = -\frac{\mathrm{i}z}{\sqrt{2\pi}fr^2}\exp\left(\mathrm{i}kr\right) \times\exp\left(-\frac{x^2+y^2}{4f^2r^2}\right)\mathrm{erf}\left(\frac{\mathrm{i}x}{2fr}\right)\mathrm{erf}\left(\frac{\mathrm{i}y}{2fr}\right), \quad (11)$$

where $f = 1/kw_0$ is the f-parameter.[3]

Using the paraxial approximation

$$r \approx z + \frac{x^2+y^2}{2z}, \quad (12)$$

we can simplify Eqs.(7) and (8) to

$$E_{f\mathrm{p}.0}(x, y, z) = E_{0\mathrm{p}}(x, y, z)\mathrm{erf}\left(\alpha_{\mathrm{p}}x\right)\mathrm{erf}\left(\alpha_{\mathrm{p}}y\right) \quad (13)$$

with

$$E_{0\mathrm{p}}(x, y, z) = \frac{1}{1+\mathrm{i}z/z_0}\frac{\sqrt{2/\pi}}{w_0}\exp\left(\mathrm{i}kz\right) \times \exp\left(\mathrm{i}k\frac{x^2+y^2}{2z}\right)\exp\left[\alpha_{\mathrm{p}}^2\left(x^2+y^2\right)\right], \quad (14)$$

$$\alpha_{\mathrm{p}} = \frac{\mathrm{i}/w_0}{\sqrt{\left(z/z_0\right)^2 - \mathrm{i}z/z_0}}, \quad (15)$$

and

$$E_{f\mathrm{p}.0}(x, y, z) = -\frac{\mathrm{i}}{\sqrt{2\pi}fz}\exp\left(\mathrm{i}kz\right)\exp\left[\frac{\mathrm{i}k}{2z}\left(x^2+y^2\right)\right]\exp\left(-\frac{x^2+y^2}{4f^2z^2}\right)\mathrm{erf}\left(\frac{\mathrm{i}x}{2fz}\right)\mathrm{erf}\left(\frac{\mathrm{i}y}{2fz}\right), \quad (16)$$

respectively. It is readily seen that Eq.(13) coincides with Eq.(14) in Ref.[2] for the case of two-dimensional paraxial free-space propagation.

If there is a knife edge offsetting from the centre of a PFG beam by a_1 and b_1 in the x and y directions, respectively, the field of the PFG beam at the plane z=0 becomes

$$E_{f.0}^{(1)}(x_0, a_1, y_0, b_1, 0) = \begin{cases} 0, & |x_0| \le a_1,\ |y_0| \le b_1, \\ \theta(x_0)\,\theta(y_0)\,E_0(x_0, y_0, 0), & |x_0| > a_1,\ |y_0| > b_1. \end{cases} \tag{17}$$

Substituting Eqs.(5) and (17) into Eq.(3), we obtain

$$E_{f.0}^{(1)}(x, a_1, y, b_1, z) = \frac{1}{4}E_0(x, y, z)\left[\mathrm{erf}(x_+^{(a_1)}) + \mathrm{erf}(x_-^{(a_1)})\right]\left[\mathrm{erf}(y_+^{(b_1)}) + \mathrm{erf}(y_-^{(b_1)})\right], \tag{18}$$

where

$$x_\pm^{(a_1)} = \alpha\left[x \pm a_1\left(1 + \mathrm{i}r/z_0\right)\right], \tag{19}$$

$$y_\pm^{(b_1)} = \alpha\left[y \pm b_1\left(1 + \mathrm{i}r/z_0\right)\right]. \tag{20}$$

Using the paraxial approximation, we can reduce Eq.(18) to

$$\begin{aligned} &E_{f\mathrm{p}.0}^{(1)}(x, a_1, y, b_1, z) \\ =&\frac{1}{4}E_{0\mathrm{p}}(x, y, z)\left[\mathrm{erf}\left(x_{p+}^{(a_1)}\right) + \mathrm{erf}\left(x_{p-}^{(a_1)}\right)\right] \\ &\times\left[\mathrm{erf}\left(y_{p+}^{(b_1)}\right) + \mathrm{erf}\left(y_{p-}^{(b_1)}\right)\right], \end{aligned} \tag{21}$$

where

$$x_{p\pm}^{(a_1)} = \alpha_{\mathrm{p}}\left[x \pm a_1\left(1 + \mathrm{i}z/z_0\right)\right], \tag{22}$$

$$y_{p\pm}^{(b_1)} = \alpha_{\mathrm{p}}\left[y \pm b_1\left(1 + \mathrm{i}z/z_0\right)\right]. \tag{23}$$

Equation (21) implies that $E_{0\mathrm{p}}(x,\, y,\, z)$ is modulated by $\left[\mathrm{erf}\left(x_{p+}^{(a_1)}\right) + \mathrm{erf}\left(x_{p-}^{(a_1)}\right)\right]$ and $\left[\mathrm{erf}\left(y_{p+}^{(b_1)}\right) + \mathrm{erf}\left(y_{p-}^{(b_1)}\right)\right]$ in the x and y directions, respectively.

Now we consider that a PFG beam propagates through a rectangular aperture with half-widths a_2 and b_2 at the plane z=0, i.e.,

$$E_{f.0}^{(2)}(x_0, a_2, y_0, b_2, 0) = \begin{cases} \theta(x_0)\,\theta(y_0)\,E_0(x_0, y_0, 0), & |x_0| \le a_2,\ |y_0| \le b_2, \\ 0, & |x_0| > a_2,\ |y_0| > b_2. \end{cases} \tag{24}$$

Recalling the relation

$$E_{f.0}^{(2)}(x_0, a_2, y_0, b_2, 0) + E_{f.0}^{(1)}(x_0, a_2, y_0, b_2, 0) \ = E_{f.0}(x_0, y_0, 0), \tag{25}$$

we obtain

$$\begin{aligned} E_{f.0}^{(2)}(x, a_2, y, b_2, z) =& E_0(x, y, z)\left\{\mathrm{erf}(\alpha x)\mathrm{erf}(\alpha y) - \frac{1}{4}\left[\mathrm{erf}\left(x_+^{(a_2)}\right) + \mathrm{erf}\left(x_-^{(a_2)}\right)\right]\right. \\ &\left.\times\left[\mathrm{erf}\left(y_+^{(b_2)}\right) + \mathrm{erf}\left(y_-^{(b_2)}\right)\right]\right\}. \end{aligned} \tag{26}$$

The corresponding paraxial propagation equation of the apertured PFG beam is given by

$$\begin{aligned} E_{f\mathrm{p}.0}^{(2)}(x, a_2, y, b_2, z) =& E_{0\mathrm{p}}(x, y, z)\left\{\mathrm{erf}\left(\alpha_{\mathrm{p}}x\right)\mathrm{erf}\left(\alpha_{\mathrm{p}}y\right) - \frac{1}{4}\left[\mathrm{erf}\left(x_{p+}^{(a_2)}\right) + \mathrm{erf}\left(x_{p-}^{(a_2)}\right)\right]\right. \\ &\left.\times\left[\mathrm{erf}\left(y_{p+}^{(b_2)}\right) + \mathrm{erf}\left(y_{p-}^{(b_2)}\right)\right]\right\}. \end{aligned} \tag{27}$$

Equations (21) and (27) coincides with Eqs.(18) and (23) in Ref.[2], respectively, for the case of two-dimensional paraxial propagation.

3. Numerical illustrative examples and discussions

Numerical calculations were made by using the formulae derived in Section 2, to illustrate nonparaxial propagation properties of PFG beams and to compare nonparaxial results with paraxial ones.

Figures 1(a) f=0.04, (b) f=0.05 and (c) f=0.30 show normalized intensity distributions $I_x/I_{x\,\max}$ of unapertured PFG beams in the x direction at the planes z=20z_0 and 40z_0, where $I_x = |E_{f.0}(x,\ 10\lambda,\ z)|^2$, $I_{x,\ \max}$ denotes the maximum intensity in the x direction. In Figs.1(a)–1(c) solid curves and circles represent the results calculated by using Eqs.(7) and (13), respectively. As can be seen, there is an on-axis central dip, i.e., $|E_{f.0}(0,\ 10\lambda,\ z)|^2$=0, and the width of the central dip increases with the increase of the distance z, which can be interpreted by using the behaviour of the error function as $|x| \to 0$ (see Appendix A). Figures 1(a) and 1(b) indicate that the paraxial approximation holds true if $f \leq 0.04$. For the case of f=0.30 in Fig.1(c) a noticeable difference between the nonparaxial and paraxial results appears. In Ref.[10] Nemoto derived the condition for the paraxial Gaussian beams, namely, $f \leq 0.18$ if the field of Gaussian beams at the plane z=0 is given by Eq.(2). It means that, as compared with Gaussian beams, for PFG beams the smaller f-parameter (i.e., the larger w_0/λ) should be taken to satisfy the paraxial approximation. In addition, numerical results by direct integration of Eq.(3) coincide with those calculated by using Eq.(7), and confirm the validity of Eq.(5).

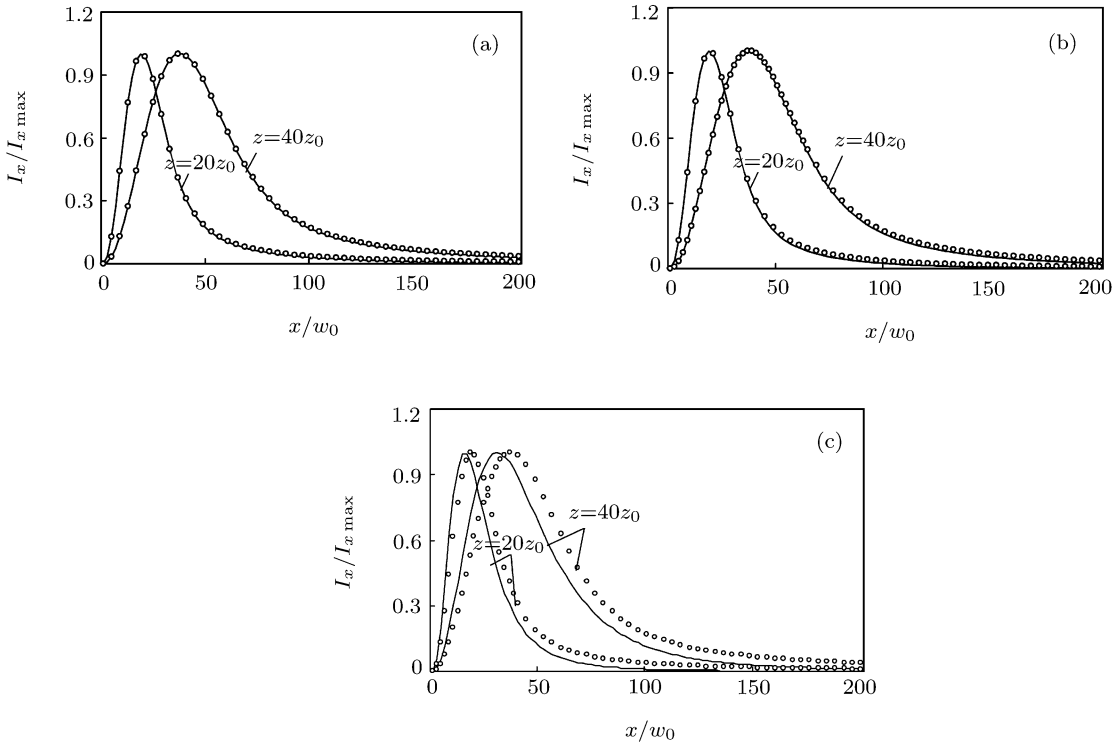


Fig.1. Normalized intensity distributions $I_x/I_{x\,\max}$ in the x direction at the plane z=20z_0 and 40z_0 of unapertured PFG beams. (a) f=0.04; (b) f=0.05, (c) f=0.30. '—', by using Eq.(7), '∘ ∘ ∘ ∘ ∘ ∘', by using Eq.(13).

Normalized intensity distributions $I_x/I_{x\,\max}$ in the x direction at the plane z=40z_0 of PFG beams with an offsetting knife edge are plotted in Figs.2(a) (f=0.04) and 2(b) (f=0.30) for different values of a_1, from which we see that the paraxial approximation is valid for $f \leq 0.04$ and $a_1 \leq 0.20w_0$. Again, an appreciable discrepancy between the results by using Eqs.(18) and (21) are seen for the case of f=0.30 in Fig.2(b).

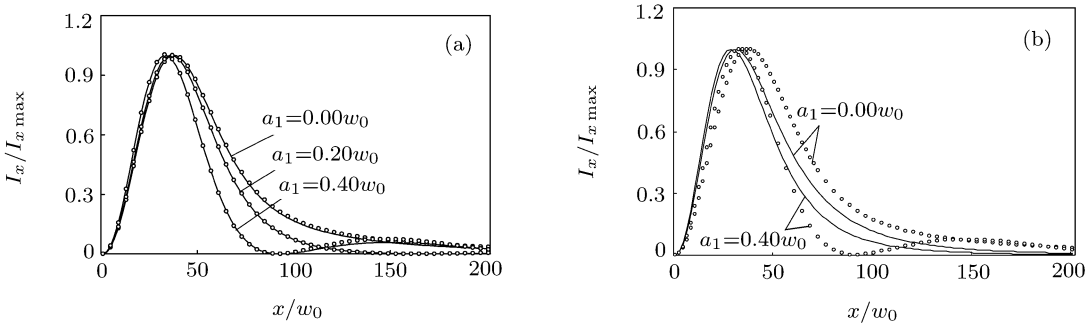


Fig.2. Normalized intensity distributions $I_x/I_{x\max}$ in the x direction at the plane z=40z_0 of PFG beams with a knife edge. (a) f=0.04; (b) f=0.30. '—', by using Eq.(18), 'o o o o o o', by using Eq.(21).

Normalized intensity distributions $I_x/I_{x\max}$ in the x direction at the plane z=40z_0 of aperture PFG beams are depicted in Figs.3(a) (f=0.04), (b) (f=0.03) and (c) (f=0.01) for different values of the truncation parameter $\delta = a_2/w_0$. Figures 3(a)–3(c) follows that the paraxial approximation is applicable under the conditions that (a) $f \leq$0.04, $\delta \geq$1.5, or (b) $f \leq$0.03, $\delta \geq$1.0, or (c) $f \leq$0.01, $\delta \geq$0.5. For the cases of (b) and (c) the aperture effect plays a role. For $\delta \geq$1.5 in Figs.3(a)–3(c) the aperture effect is negligible because for such cases the use of Eqs.(7) and (26) delivers the same result. The aperture half-width a_2, with which the PFG beams remain effectively unapertured, increases as the f parameter decreases, because the beam width increases with decreasing f parameter.

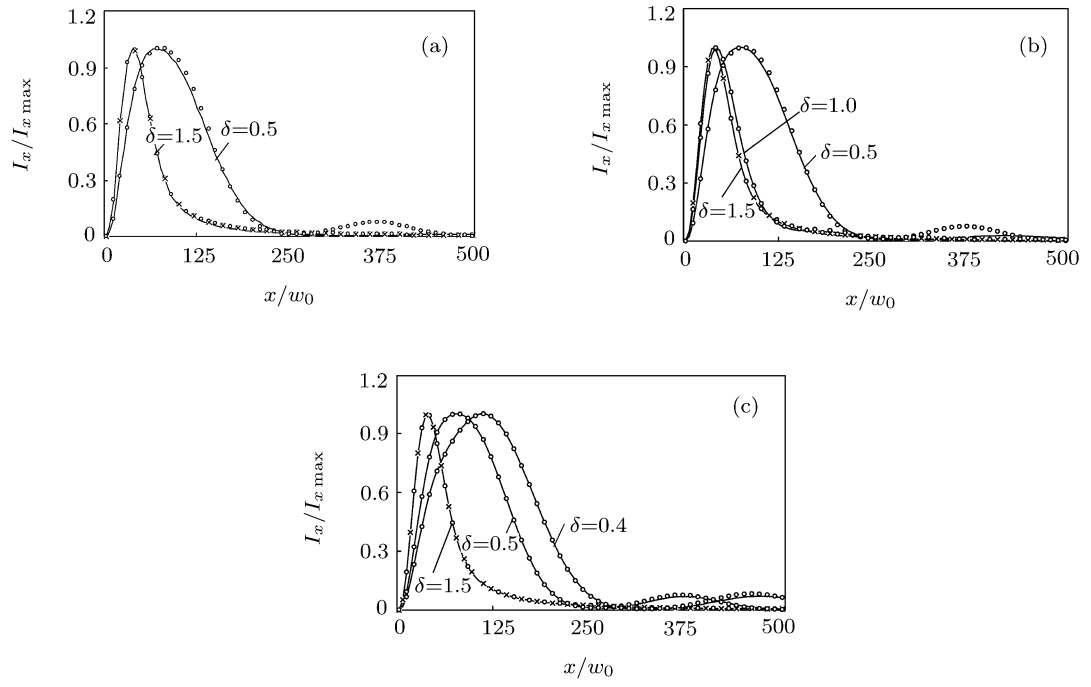


Fig.3. Normalized intensity distributions $I_x/I_{x\max}$ in the x direction at the plane z=40z_0 of apertured PFG beams. f=0.04, (b) f=0.03, (c) f=0.01. '—', by using Eq.(26), 'o o o o o o', by using Eq.(27), '× × × × ××', by using Eq.(7).

4. Concluding remarks

In this paper, based on the Rayleigh–Sommerfeld diffraction integral, analytical expressions for nonparaxial PFG beams propagating in free space and through a knife edge and an aperture have been derived. Just like the paraxial case, the propagation equations are written as a product of two terms—one of them is the free-space propagation expression

of nonparaxial Gaussian beams and the other term is the complex-argument error function. The latter term describes the modulation due to the flipped phase, offsetting knife edge and aperture. Under the paraxial approximation our formulae reduce to the corresponding paraxial ones. The f parameter, offsetting distance and truncation parameter affect the nonparaxial propagation behaviour of PFG beams. Only under certain conditions, e.g., for $f \leq 0.04$ in the free-space propagation case; $f \leq 0.04$, and $a_1 \leq 0.20 w_0$ in the offsetting knife edge case, and $f \leq 0.03$, $\delta \geq 1.0$ in the apertured case, the paraxial approximation is valid. Otherwise, the nonparaxial approach in this paper should be taken.

Appendix A

The error function $\mathrm{erf}(x)$ can be approximately expressed as

$$\mathrm{erf}(x) \approx \frac{2x}{\sqrt{\pi}} + O(x^3) \quad \text{for} \quad |x| \to 0 \tag{A1}$$

and

$$\mathrm{erf}(x) \approx 1 - \frac{\exp(-x^2)}{x\sqrt{\pi}}(1 + O(x^{-x^2})) \quad \text{for} \quad |x| \gg 1 \quad \text{and} \quad \mathrm{Re}x \geq 0. \tag{A2}$$

Therefore, for $x^2 \ll \frac{r}{z_0}\sqrt{1+\left(\frac{r}{z_0}\right)^2}$ the use of Eq.(A1) in Eq.(7) yields

$$|E_{f.0}(x,y,z)|^2 \approx \frac{32}{\pi^3 w_0^4}\frac{z^2 z_0^2/r^4}{(1+r^2/z_0^2)^2}x^2y^2 \times \exp\left[\frac{-2\left(x^2+y^2\right)}{w_0^2(1+r^2/z_0^2)}\right]. \tag{A3}$$

Equation (A3) indicates that $|E_{f.0}(x,y,z)|^2 \approx 0$ as $|x| \to 0$, and for a given value of x near $x=0$, $|E_{f.0}(x,y,z)|^2$ decreases with an increase of z, which results in an widening of the on-axis dip.

On the other hand, for $\frac{x^2}{w_0^2} \gg \frac{r}{z_0}\sqrt{1+\left(\frac{r}{z_0}\right)^2}$, the use of Eq.(A2) in Eq.(7) leads to

$$|E_{f.0}(x,y,z)|^2 \approx \frac{2}{\pi}\frac{z^2/r^2}{1+r^2/z_0^2}\exp\left[\frac{-2\left(x^2+y^2\right)}{w_0^2(1+r^2/z_0^2)}\right]\left[1+\chi_{x0}^2+2\chi_{x0}\sin\psi_{x0}\right]\left[1+\chi_{y0}^2+2\chi_{y0}\sin\psi_{y0}\right], \tag{A4}$$

where

$$\chi_{\beta 0} = \sqrt{\frac{r/z_0}{\pi\beta^2/w_0^2}}\left(1+r^2/z_0^2\right)^{1/4}\exp\frac{\beta^2/w_0^2}{1+r^2/z_0^2}, \quad (\beta = x, y), \tag{A5}$$

$$\psi_{\beta 0} = \frac{\beta^2/w_0^2}{r/z_0\left(1+r^2/z_0^2\right)} - \frac{1}{2}\arctan\left(\frac{1}{r/z_0}\right), \quad (\beta = x, y). \tag{A6}$$

From Eq.(A4) it follows that the oscillation may appear because Eq.(A4) contains sin terms.

Similarly, for the offsetting knife edge case, we obtain

$$\left|E_{f.0}^{(1)}(x,a_1,y,b_1,z)\right|^2 \approx \frac{2}{\pi^3 w_0^4}\frac{z^2 z_0^2/r^4}{(1+r^2/z_0^2)^2}x^2y^2\exp\left[\frac{-2\left(x^2+y^2\right)}{w_0^2(1+r^2/z_0^2)}\right] \quad \text{for} \quad (x\pm a_1)^2 + \frac{r^2a_1^2}{z_0^2} \ll \frac{r}{z_0}w_0^2\sqrt{1+\left(\frac{r}{z_0}\right)^2} \tag{A7}$$

and

$$\left|E_{f.0}^{(1)}(x,a_1,y,b_1,z)\right|^2 \approx \frac{2}{\pi}\frac{z^2/r^2}{1+r^2/z_0^2}\exp\left[\frac{-2\left(x^2+y^2\right)}{w_0^2(1+r^2/z_0^2)}\right]A_xA_y \quad \text{for} \quad (x\pm a_1)^2 + \frac{r^2a_1^2}{z_0^2} \gg \frac{r}{z_0}w_0^2\sqrt{1+\left(\frac{r}{z_0}\right)^2}, \tag{A8}$$

where

$$A_\beta = 1 + \left(\chi_{\beta+}^2 + \chi_{\beta-}^2\right)/4 + \left(\chi_{\beta+}\chi_{\beta-}/2\right)\cos\left(\psi_{\beta-} - \psi_{\beta+}\right) + \left(\chi_{\beta+}\sin\psi_{\beta+} + \chi_{\beta-}\sin\psi_{\beta-}\right), \quad \beta = x, y, \tag{A9}$$

$$\chi_{x\pm} = \frac{\sqrt{r/z_0}\left(1+r^2/z_0^2\right)^{1/4}}{\sqrt{\pi}(z\pm a_1)/w_0}\exp\left[\frac{(x\pm a_1)^2/w_0^2}{1+r^2/z_0^2}\right], \tag{A10}$$

$$\chi_{y\pm} = \frac{\sqrt{r/z_0}\left(1+r^2/z_0^2\right)^{1/4}}{\sqrt{\pi}(z\pm b_1)/w_0}\exp\left[\frac{(y\pm b_1)^2/w_0^2}{1+r^2/z_0^2}\right], \tag{A11}$$

$$\psi_{x\pm} = \frac{(x\pm a_1)^2/w_0^2}{r/z_0\left(1+r^2/z_0^2\right)} - \frac{1}{2}\arctan\left(\frac{1}{r/z_0}\right), \tag{A12}$$

$$\psi_{y\pm} = \frac{(y\pm b_1)^2/w_0^2}{r/z_0\left(1+r^2/z_0^2\right)} - \frac{1}{2}\arctan\left(\frac{1}{r/z_0}\right). \tag{A13}$$

Using the paraxial approximation, it is readily seen that Eqs.(A3), (A4) and (A8) reduce to Eqs.(28), (29) and (34) in Ref.[2], respectively for the two-dimensional paraxial case.

References

[1] Delaubert V, Shaddock D A, Lam P K, Buchler B C, Bachor H-A and Mc Clelland D E 2002 *J. Opt.* A: *Pure Appl. Opt.* **4** 393

[2] Banerji J 2006 *Opt. Commun.* **258** 1

[3] Lax M, Louisell W H and McKnight W B 1975 *Phys. Rev.* A **11** 1365

[4] Agrawal G P and Pattanatak D N 1979 *J. Opt. Soc. Am.* A **68** 575

[5] Liu P S and Lü B D 2004 *Acta Phys. Sin.* **53** 3724 (in Chinese)

[6] Duan K L and Lü B D 2004 *Opt. & Laser. Tech.* **36** 489

[7] Gao Z H and Lü B D 2006 *Chin. Phys.* **15** 334

[8] Zeng X, Liang C and An Y 1999 *Appl. Opt.* **36** 6253

[9] Luneberg R K 1996 *Mathematical Theory of Optics* (Berkeley, CA: University of California Press)

[10] Nemoto S 1990 *Appl. Opt.* **29** 1940